

Natural Convection in a Horizontal Cylindrical Annulus with Two Isothermal Blocks in Median Position: Numerical Study of Heat Transfer Enhancement

S. Touzani, A. Cheddadi[†] and M. T. Ouazzani

Research Team, Energy systems, Mechanical structures and Materials, and Industrial Processes modeling, MOSEM2PI, Mohammadia School of Engineers, Mohammed V University in Rabat, P. O. Box 765 Agdal, Rabat, Morocco

[†]Corresponding Author Email: cheddadi@emi.ac.ma

(Received January 25, 2019; accepted June 21, 2019)

ABSTRACT

Natural convection is numerically investigated in a finned horizontal cylindrical annulus filled with air where two isothermal blocks are attached to the inner cylinder in a median position. A bi-vortex flow is observed and the influence of each vortex on heat transfer is analysed. Heat flux and transfer rate calculated per zone (superior, central and inferior) show that heat transfer is more important for the annulus superior zone. Compared to without blocks configuration, blocks presence contributes in the overall heat transfer improvement. This improvement is observed at the inferior zone (inferior vortex effect) and the central one. For the superior zone, despite its importance, heat transfer is deteriorated. This study also shows that the addition of inverted trapezoidal blocks to the medium increases heat transfer, relatively to the without blocks case, by 10.54% to 29.62% depending on Rayleigh number.

Keywords: Natural convection; Horizontal annulus; Isothermal blocks; Median position; Heat transfer rate.

NOMENCLATURE

g	gravitational acceleration	η	efficiency
h	dimensionless block's height	φ	polar angle
l	dimensionless block's width	ϕ	heat flux
\overline{Nu}	overall Nusselt number	φ_m	block's angular position
Pr	Prandtl number	ψ	dimensionless stream function
R	radius ratio	ω	dimensionless vorticity
r	dimensionless coordinate		
r'_i	inner cylinder radius	Subscripts / Exponents	
r'_o	outer cylinder radius	i	inner
Ra	Rayleigh number	o	outer
T'_i	inner cylinder temperature	max	maximum.
T'_o	outer cylinder temperature	'	dimensional value
u	dimensionless radial velocity	0	without blocks case
v	dimensionless angular velocity	inf	inferior zone
ν	kinematic viscosity	cent	central zone
		sup	superior zone
α	thermal diffusivity		
β	thermal expansion coefficient		

1. INTRODUCTION

Producing economical heating and cooling systems with high performances is a constant concern in the

industry. One of the phenomena that occurs and achieves those goals is natural convection. Natural convection in annuli has specially attracted researchers' attention due to its various industrial

and technological applications such as heat exchangers, thermal storage systems and electronic devices cooling (Dawood *et al.*, 2015). For decades, natural convection in horizontal concentric annulus without fins was first investigated (Cheddadi *et al.*, 1992; Yoo, 1999; Mizushima *et al.*, 2001; Volkov and Karpenko, 2014). Then lately, other shapes of annulus were studied (Ahmed and Ahmed, 2017). Some authors were interested in modifying the inner geometry of the horizontal concentric annulus. Sheikholeslami *et al.* (2013) conducted a numerical investigation of natural convection in an annulus where the inner enclosure is sinusoidal. Many parameters such as the Rayleigh number, the value of amplitude and the number of undulations of the inner cylinder were studied. Yuan *et al.* (2015) changed the shape of the inner entity of the concentric annulus into cylindrical, elliptical, square or triangular forms and analysed the effects of this variation on flow pattern and heat transfer distribution. The presence of corners in the square and triangular annuli and the larger top in the elliptical annulus was found to enhance heat transfer performance as compared to the concentric cylindrical annulus. Those inner entity changes can be assimilated to fins which are utilized frequently to extend the surface of contact with the fluid and increase the heat transfer rate as Nagarani *et al.* (2014) mentioned in their review. Fins orientation, number, shape, spacing and arrangement were the subject of many investigations (Chai and Patankar, 1993; Farinas *et al.*, 1997; Rahnama *et al.*, 1999; Kundu, 2015; Iqbal *et al.*, 2011; Zhang *et al.*, 2012; Ishaq *et al.*, 2013; Arbaban and Salimpour, 2014; Kundu, 2015; Kumar *et al.*, 2015). In addition, certain authors were interested in the fins inclination angle. Rahnama and Farhadi (2004) began by investigating the impact of two radial fins, attached to the inner cylinder of a horizontal annulus, located in the middle of the geometry, on heat transfer rate and flow pattern before adding more fins and changing their arrangements. Alshahrani and Zeitoun (2005) also studied two fins placed in the middle of a horizontal annulus then changed the fins position, their height and the annulus radii ratio. In these studies, fins have a constant thin thickness. When the fin thickness is slightly important, the name of blocks is adopted instead of fins (Bakkas *et al.*, 2010; Ould-Amer, 2016). Charles and Wang (2014) compared various fin assembly of a heat sink with rectangular, trapezoidal and inverted trapezoidal fin configuration. They found that the inverted trapezoidal fin configuration is better than the others. Idrissi *et al.* (2016) adopted this block geometry and inserted two isothermal blocks with low heights symmetrically in the upper zone of a horizontal annulus filled with air. As a result, they detected a bifurcation point separating unicellular and bicellular flows and found that the bicellular flow improves the heat transfer rate. They also studied initial conditions influence on low and median block positions with low block heights.

Optimizing the blocks or fins parameters is still intriguing despite the considerable amount of works already published. In the present paper, the inverted

trapezoidal shape is adopted for two isothermal blocks, with medium height, placed in a median position on the inner cylinder of a horizontal annulus filled with air. It is intended to examine their influence on both heat transfer rate and flow pattern by comparing the results to those obtained without blocks. An analysis of heat transfer per zone within the annular cavity is also proposed.

2. PROBLEM STATEMENT

The system consists of two extremely long horizontal coaxial cylinders with inner and outer cylinders of radii r'_i and r'_o , held at temperatures T'_i and T'_o respectively with $T'_o < T'_i$ (Fig. 1). The annular cavity is filled by air considered as an incompressible Newtonian fluid ($Pr = 0.7$). Two isothermal blocks of height h' and width l' are placed on the hot wall in the middle part of the annular space, symmetrically with respect to the vertical plane containing the cylinders axis. In this work, the blocks have dimensionless height h relative to the inner radius r'_i and width l related to the inner half - perimeter ($\pi r'_i$). The blocks position is fixed in a median position defined by the angular

position φ_m as $\varphi_m = \frac{\varphi_{inf} + \varphi_{sup}}{2}$ where φ_{inf} and

φ_{sup} are the polar angles limiting the blocks calculated from the space bottom. The radius ratio $R = r'_o / r'_i$, the dimensionless height and width of the blocks are kept constant throughout the study to $R = 2$, $h = 0.5$ and $l = 0.109$ respectively. The studied zones are also presented. Inferior, central and superior zones are determined by the intervals $0 \leq \varphi < \varphi_{inf}$, $\varphi_{inf} \leq \varphi \leq \varphi_{sup}$ and $\varphi_{sup} < \varphi \leq \pi$ respectively.

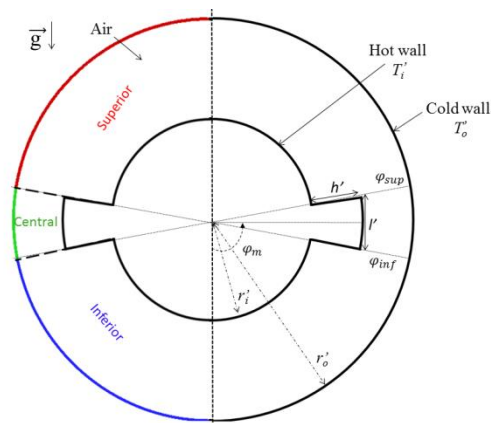


Fig. 1. Horizontal annulus scheme with two blocks.

The Boussinesq approximation is assumed and the stream function-vorticity formulation is adopted. The governing equations for two-dimensional flow are written in dimensionless form, as the following:

$$\Delta\psi + \omega = 0 \tag{1}$$

$$\frac{\partial \omega}{\partial t} + \frac{1}{r} \left(\frac{\partial \psi}{\partial \varphi} \frac{\partial \omega}{\partial r} - \frac{\partial \psi}{\partial r} \frac{\partial \omega}{\partial \varphi} \right) = \text{Pr} \Delta \omega + Ra \text{Pr} \left(\frac{\cos \varphi}{r} \frac{\partial T}{\partial \varphi} + \sin \varphi \frac{\partial T}{\partial r} \right) \quad (2)$$

$$\frac{\partial T}{\partial t} + \frac{1}{r} \left(\frac{\partial \psi}{\partial \varphi} \frac{\partial T}{\partial r} - \frac{\partial \psi}{\partial r} \frac{\partial T}{\partial \varphi} \right) = \Delta T \quad (3)$$

where the dimensionless variables are:

$$r = r'/r'_i, \quad t = (\alpha / r'_i{}^2) t', \quad \psi = \psi' / \alpha, \\ \omega = (r'_i{}^2 / \alpha) \omega' \\ \text{and } T = (T' - T'_o) / (T'_i - T'_o).$$

Two dimensionless parameters surface up in the Eq. (2):

$$\text{Rayleigh number: } Ra = \beta g (T'_i - T'_o) r'_i{}^3 / \nu \alpha \quad \text{and} \\ \text{Prandtl number: } Pr = \nu / \alpha.$$

The dimensionless boundary conditions are given as below:

- On the inner cylinder: $r = 1, 0 \leq \varphi \leq \varphi_{inf}$ and

$$\varphi_{max} \leq \varphi \leq \pi : \psi = 0, \quad \frac{\partial \psi}{\partial r} = 0, \\ \frac{\partial^2 \psi}{\partial r^2} + \omega = 0, \quad T = 1 \quad (4)$$

- On the blocks surfaces:

$$r = 1+h \text{ and } \varphi_{inf} \leq \varphi \leq \varphi_{sup} : \psi = 0, \quad \frac{\partial \psi}{\partial r} = 0, \\ \frac{\partial^2 \psi}{\partial r^2} + \omega = 0, \quad T = 1. \quad (5)$$

$$\varphi = \varphi_{inf} \text{ and } \varphi = \varphi_{sup}, 1 \leq r \leq h+1 :$$

$$\psi = 0, \quad \frac{\partial \psi}{\partial \varphi} = 0, \quad \frac{1}{r^2} \frac{\partial^2 \psi}{\partial \varphi^2} + \omega = 0, \quad T = 1. \quad (6)$$

- On the outer cylinder: $r = R: \psi = 0, \frac{\partial \psi}{\partial r} = 0,$

$$\frac{\partial^2 \psi}{\partial r^2} + \omega = 0, \quad T = 0 \quad \forall \varphi \quad (7)$$

Due to the symmetry of the problem, these equations will be solved only for the half of the cavity. Therefore, additional boundary conditions are taken into account:

- $\varphi = 0, \varphi = \pi : \psi = 0, \omega = 0, \frac{\partial T}{\partial \varphi} = 0 \quad \forall r \quad (8)$

The system of equations with boundary conditions (1-8) is numerically solved by centred finite difference using the ADI scheme (Alternating Direction Implicit). The considered solutions are obtained when steady state regimes are established.

In this work, the considered initial conditions are based on pure conduction profile of temperature with stream-function and vorticity fields equal to

zero.

The computational code has been validated by comparing the overall heat transfer rates of $h = 0$ case and the without blocks code developed by [Cheddadi *et al.* \(1992\)](#) using artificial compressibility with primitive variables. The relative difference between overall heat transfer rates does not exceed 0.24% found for $Ra = 10000$.

Grid sensitivity was examined by solving the present problem for different meshes. By refining the grid size, negligible changes on the results were noticed from 65×65 mesh. Therefore, this mesh size can be considered sufficient to describe the obtained solutions. Converged solutions were obtained when the relative difference between the calculated parameters and their values in the previous iteration step, at any point in the domain, remained close to 10^{-6} .

3. RESULTS AND DISCUSSION

The results are presented for a block, of a height $h = 0.5$, placed in a median position $\varphi_m = 0.49\pi$ in the half of the cavity and for Rayleigh numbers range varying between 1000 and 10000. Flow intensity, local and overall Nusselt numbers and heat flux are calculated for both configurations with and without blocks, this latter appointed by the exponent 0.

3.1 Flow Pattern and Isotherms

Figure 2 shows that the isotherms are globally similar for both configurations. For $Ra = 1000$, they are almost concentric in the annulus with a slight stratification near the tangential side of the block. By increasing Rayleigh number, they become more deformed and distorted in the medium for both configurations. A thermal plume is observed on the upper part of the annulus for high Ra . However, the flow structure of each configuration is different. For the without blocks case, unicellular flow is observed in [Cheddadi *et al.* \(1992\)](#), [Volkov *et al.* \(2014\)](#) and [Yuan *et al.* \(2015\)](#) for the same fixed parameters of this study. For the with blocks configuration, the observed flow pattern is a bi-vortex flow where one cell contains two vortices rotating in the same direction. This flow structure has already been pointed out by [Ha and Kim \(2004\)](#) for fins with medium height arranged in '+' shape and by [Alshahrani and Zeitoun \(2005\)](#) when they placed two thin fins with medium height in a median position.

The two superior and inferior vortices have almost the same size due to the division of the medium to two equal spaces. However, their intensities $\psi_{max\ sup}$ and $\psi_{max\ inf}$ are quite different (Fig. 3). We observe that $\psi_{max\ sup} > \psi_{max\ inf}$, meaning that the superior vortex has a greater intensity than that of the inferior one despite the similarity of their shape. Thus, no direct link exists between the vortex size and its intensity. In fact, at the block level, a hot current stream from the inferior zone contributes in increasing the heating of the fluid in the superior

zone, causing the acceleration of its movement and therefore forming an intense superior vortex. In contrary, the fluid in the inferior annulus region is cooled because of the downward flow along the cold wall which slows down the inferior vortex circulation. We also notice that the maximum intensities of the without blocks configuration, for the two superior and inferior zones, $\psi^0_{max\ sup}$ and $\psi^0_{max\ inf}$ are always greater than those of with blocks configuration, $\psi_{max\ sup}$ and $\psi_{max\ inf}$ respectively. Unlike the without blocks case, where the fluid moves freely, the flow recirculation is slowed down because of the blocks presence. This fact was also noticed by [Chai and Patankar \(1993\)](#) and [Rahnama *et al.* \(1999\)](#) using different fins arrangements.

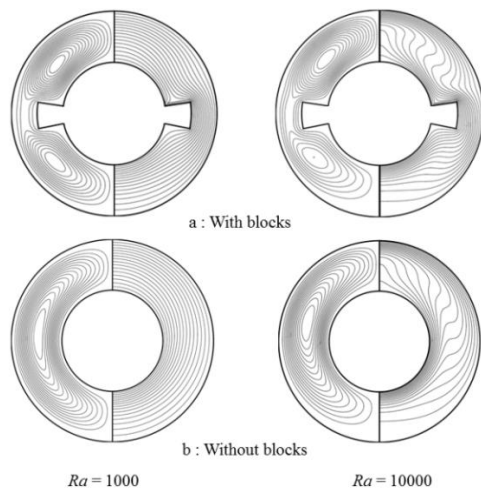


Fig. 2. Streamlines (left) and isotherms (right) for the two studied configurations at $Ra = 1000$ and $Ra = 10000$. a: with blocks, b: without blocks.

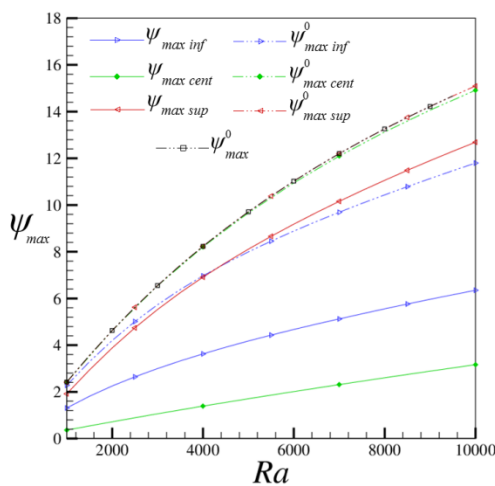


Fig. 3. Intensities ψ_{max} for different Rayleigh numbers.

The intensities of the three considered zones in the present work, for with and without blocks configurations, increase naturally with Ra

augmentation. Actually, the one cell found in the without blocks case is characterized by an intensity ψ^0_{max} which is equal to $\psi^0_{max\ sup}$ especially from $Ra = 2500$ due to the shift of the cell centre to the superior zone when Ra increases.

3. 2 Local heat transfer and efficiency:

The local heat transfer through the cold wall represented by the local Nusselt number is defined by the expression: $Nu = -R \ln R \left. \frac{\partial T}{\partial r} \right|_{r=R}$. The overall

heat transfer in the medium translated by the overall Nusselt number is calculated by integrating Nu across the entire domain: $\overline{Nu} = \frac{-R \ln R}{\pi} \int_0^\pi \left. \frac{\partial T}{\partial r} \right|_{r=R} d\varphi$.

In the with blocks case, Nu curves as a function of φ for the different studied Rayleigh numbers are plotted in Fig. 4 which shows that we can distinguish three intervals of φ . For $\varphi < 0.24\pi$ and $\varphi > 0.68\pi$, no crossing between these curves is noticed. They are ordered as Nu decreases with Ra augmentation for the first interval and inversely for the second. For $0.24\pi \leq \varphi \leq 0.68\pi$, three crossings of those curves are observed with successive changes in their order of variation as a function of Ra . The first crossing occurs, regardless of Ra , at a quasi-constant value of $\varphi = 0.24\pi$. The other crossings occur in a range of φ between 0.39π and 0.68π depending on Ra . Nu curves as a function of φ have two maximums: a first maximum localised at $\varphi_{1st\ max}$ and a second one at $\varphi_{2nd\ max} = \pi$ (Table 1). Concerning $\varphi_{1st\ max}$, it is situated between φ_{inf} and φ_m for $Ra \leq 2000$ and decreases when Ra increases to become inferior to φ_{inf} . In fact, one of those extremums is the absolute maximum of Nu depending on Rayleigh number, observed at $\varphi_{abs\ max} = \varphi_{1st\ max}$ for $Ra \leq 2000$ and $\varphi_{abs\ max} = \varphi_{2nd\ max}$ for $Ra \geq 3000$ as illustrated in Fig. 5.

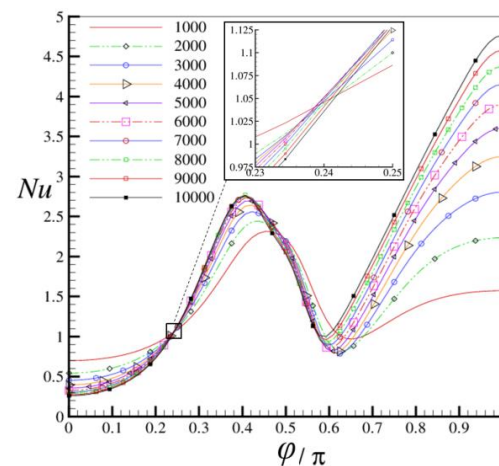


Fig. 4. Variation of Nu as a function of φ for different Ra .

Table 1 Positions of Nu maximums and absolute maximums depending on Ra

Ra	$\varphi_{1st\ max}$	$\varphi_{2nd\ max}$	$\varphi_{abs\ max}$
1000	0.45π	π	0.45π
2000	0.437π	π	$0.437\pi = \varphi_{inf}$
3000	0.42π	π	π
4000	0.42π	π	π
5000-10000	0.406π	π	π

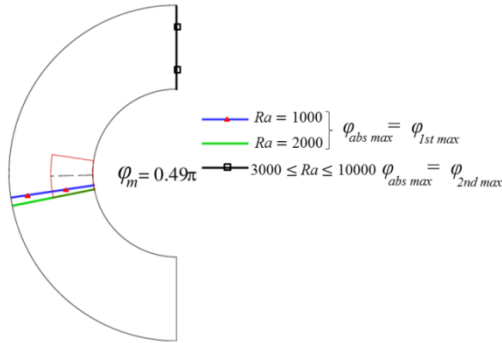


Fig. 5. Nu absolute maximums positions depending on Ra .

Regardless of Ra , Nu^0 increases with φ augmentation for the without blocks configuration, showing the importance of heat transfer at the annulus superior zone compared to its inferior one, with a maximum always observed at $\varphi = \pi$ (Fig. 6). For a given position φ , the relative difference between Nu and Nu^0 , representing local thermal efficiency, is defined by: $\eta_l = \frac{Nu - Nu^0}{Nu^0}$ (Fig. 7).

We notice that for all Rayleigh numbers, η_l is positive for a range of φ between 0 and values depending on Ra varying between 0.53π and 0.59π with a maximum of 148.13% at $\varphi = 0.437\pi$ for $Ra = 1000$ and 206.55% at $\varphi = 0.344\pi$ for $Ra = 10000$, meaning that heat transfer is always improved in the lower half of the medium. This local efficiency increase is mainly related to the heating block presence (as shown by the positioning of the first maximum of Nu curves as a function of φ at the block vicinity) and not to the effect of the intensity (indeed, $\psi_{max\ inf}^0 > \psi_{max\ inf}$). Then, heat transfer deteriorates; η_l becomes negative up to limit values: -21.56% for $Ra = 1000$ at $\varphi = 0.656\pi$ and -52.72% for $Ra = 10000$ at $\varphi = 0.594\pi$, to then increase to values between -0.53% and 5.70% respectively. This heat transfer deterioration compared to the without blocks case is due to the slowing effect of the convective flow in the superior zone by the block which hinders the motion of the fluid coming from the inferior zone ($\psi_{max\ sup}^0 > \psi_{max\ sup}$, Fig. 3).

In the following sections, we are interested in studying the influence, as a function of Ra , of the

three superior, central and inferior zones, on the heat flux and overall transfer rate on the outer wall.

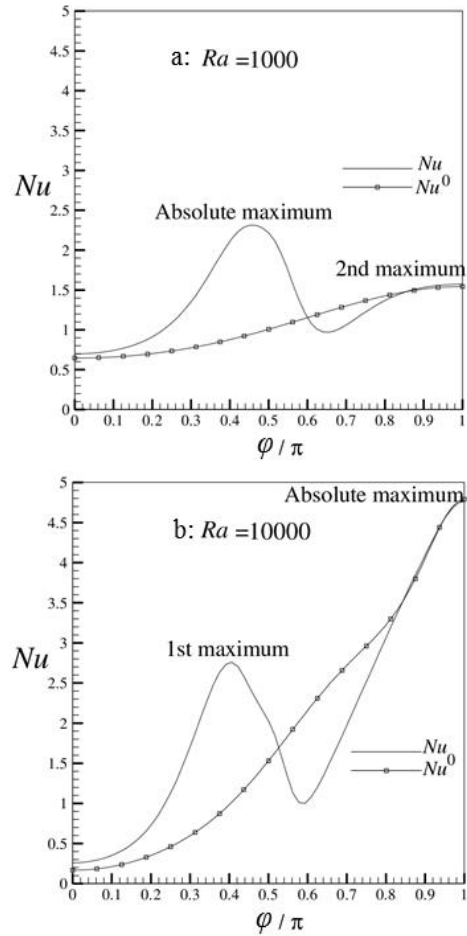


Fig. 6. Variation of Nu and Nu^0 as a function of φ . a: $Ra = 1000$. b: $Ra = 10000$.

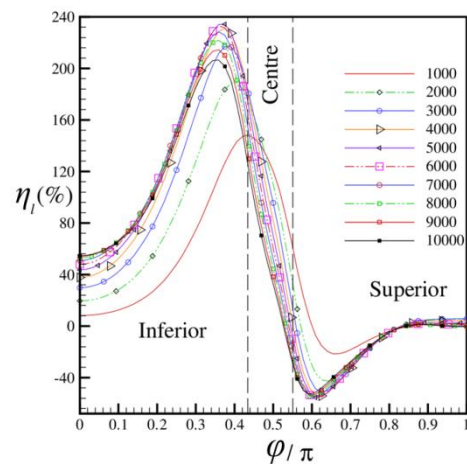


Fig. 7. Local efficiency as a function of φ for different Ra .

3.3 Heat Flux

The contribution in terms of heat transfer of the

three zones: inferior ($0 \leq \varphi < 0.437\pi$), central ($0.437\pi \leq \varphi \leq 0.55\pi$) and superior ($0.55\pi < \varphi \leq \pi$) is evaluated by calculating the heat flux through the cold wall, defined according to the considered zone

by: $\phi = -R \ln R \int \frac{\partial T}{\partial r} \Big|_{r=R} d\varphi$. Globally, the heat flux

ϕ calculated over the entire outer wall for with blocks configuration is higher than the one of the without blocks case ϕ^0 . The fluxes variation as a function of Ra for the different considered zones, allows us to notice that, whatever Ra , ϕ_{sup} of the superior zone is greater than ϕ_{inf} and ϕ_{cent} of the inferior and central zones respectively with ϕ_{cent} being the weakest (Fig. 8). Thus, the contribution in terms of heat transfer of the superior zone relatively to the entire outer wall, is the most important regardless of Ra and varies from 43.66% for $Ra = 1000$ to 62.78% for $Ra = 10000$. The inferior and central zones contributions decrease from 36.73% to 24.82% and from 19.61% to 12.40% respectively for $Ra = 1000$ and $Ra = 10000$. The significant contribution of the superior zone in terms of heat transfer can be justified by the importance of the convective flow translated by the high intensity of the superior vortex in this zone ($\psi_{max\ sup} > \psi_{max\ inf}$), already shown in Fig. 3.

Indeed, we are witnessing an acceleration of the ascending fluid heated by both the inlet wall of the cavity and the block, thereby promoting heat transfer at the superior zone. Downward to the central zone, the fluid cools and the relatively small exchange surface explains the weak flux crossing this zone. This flux is even lower than the one of the inferior zone.

In fact, in the inferior zone, in addition to the larger exchange surface than that of the central zone, the recirculation of a part of the hot flow carried almost directly from the inner to the outer cylinder allows heat transfer increase in this area.

Similarly to the discrepancy observed between $\psi_{max\ sup}$ and $\psi_{max\ inf}$, the gap between ϕ_{sup} and ϕ_{inf} is relatively small for $Ra \leq 2000$. However, for $Ra \geq 3000$, this gap becomes larger with the increase of Ra thanks to the developed convective circulation in the superior zone and to the position of Nu second maximum obtained at $\varphi = \pi$.

We also notice that the fluxes ϕ_{inf} and ϕ_{cent} are greater than ϕ_{inf}^0 and ϕ_{cent}^0 for the respective inferior and central zones contrarily to the superior zone where the opposite is observed ($\phi_{sup}^0 > \phi_{sup}$).

In the superior zone, the downward fluid is cooled by the cold wall and partially returns to the hot wall through the superior vortex. This recirculation of the fluid not completely cooled is characterized by heat transfer deterioration compared to without blocks case, where the fluid continues to cool down all the way through the cold wall. This is illustrated

by the relatively large spacing of the isotherms around 0.6π , observed for $Ra = 10000$ in Fig. 2, explaining the local Nusselt number decrease in that region shown in Fig. 6.

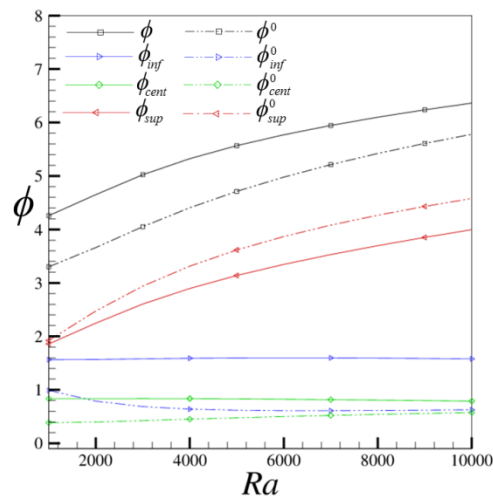


Fig. 8. Flux variation as a function of Ra for the three zones: superior, central and inferior.

3.4 Nusselt Number and Overall Efficiency

Figure 9 gives the variation as a function of Ra of the overall Nusselt number \overline{Nu} calculated on the entire cold wall, plus the average Nusselt numbers \overline{Nu}_{sup} , \overline{Nu}_{cent} and \overline{Nu}_{inf} calculated on the three superior, central and inferior zones respectively. We observe that \overline{Nu} and \overline{Nu}_{sup} increase with the augmentation of Ra . On the other side, \overline{Nu}_{inf} remains almost constant despite the heating effect from both the block and Rayleigh number increase. This effect is compensated by the local heat transfer decrease in the entire zone of $\varphi \leq 0.24\pi$ (Fig. 4), where a stagnant region is remarked as for the without blocks case, a fact previously observed for this latter case by Cheddadi *et al.* (1992). Nusselt number of the central zone \overline{Nu}_{cent} remains almost constant then slightly decreases. Comparing those Nusselt numbers with each other, we notice that the average Nusselt number \overline{Nu}_{sup} related to the superior vortex always remains, regardless of Ra , greater than \overline{Nu}_{inf} as it is the case for the flux. Nusselt number \overline{Nu}_{cent} , related to the heating generated by the block, is the most important for $Ra < 4750$ and remains almost constant. Beyond this value, \overline{Nu}_{sup} , which increases as a function of Ra , becomes the most important and strongly influences the average heat transfer increase.

Regarding the without blocks configuration, the ascending convective flow, more and more intense and hot, involves an average Nusselt number, \overline{Nu}_{sup}^0 calculated on the superior zone always greater than \overline{Nu}_{cent}^0 and \overline{Nu}_{inf}^0 regardless of Ra .

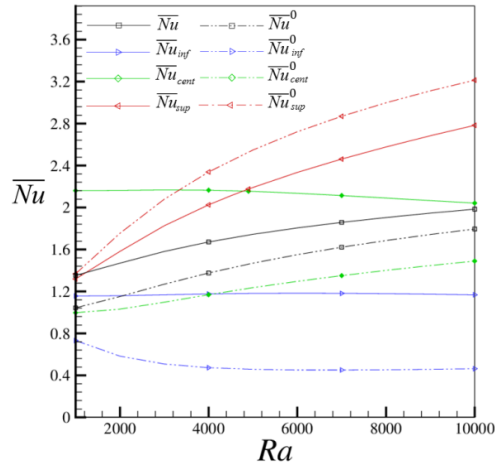


Fig. 9. \overline{Nu} variation as a function of Ra through the three zones.

We are interested then in determining the gain in terms of heat transfer observed between the cases with and without blocks, evaluated by the following expressions of the efficiencies for the three zones:

$$\eta_{sup} = \frac{\overline{Nu}_{sup} - \overline{Nu}_{sup}^0}{\overline{Nu}_{sup}^0}, \quad \eta_{cent} = \frac{\overline{Nu}_{cent} - \overline{Nu}_{cent}^0}{\overline{Nu}_{cent}^0},$$

$$\eta_{inf} = \frac{\overline{Nu}_{inf} - \overline{Nu}_{inf}^0}{\overline{Nu}_{inf}^0} \quad \text{and for the overall efficiency}$$

$$\text{given by: } \eta = \frac{\overline{Nu} - \overline{Nu}^0}{\overline{Nu}^0}.$$

The η_{inf} curve as a function of Ra shows that heat transfer in the inferior zone is remarkably improved especially for high Rayleigh numbers around $Ra > 4500$ (Fig. 10). Whence, even if the influence of the inferior vortex is the lower in intensity and heat transfer compared to the superior vortex, its role related to the heating effect in the with blocks case is reinforced compared to thermal exchanges in the lower part of the without blocks medium. In the central zone, heat transfer is highly improved specially for low Ra values, $Ra \leq 2000$. We also notice that η_{cent} decreases despite the increase of Ra , translating the blocking effect of the flow by the block. Moreover, in the superior zone, heat transfer is deteriorated with $\eta_{sup} < 0$ regardless of Ra .

Despite the fact that the intensities of the two vortices in with blocks configuration are lower than that of the without blocks configuration flow, the presence of the block improves the overall heat transfer which is translated by $\eta > 0$ in Fig. 10. The competition between the two roles played by the block, namely flow hindrance and heating, favours this enhancement. The increase of Ra reduces constantly the overall efficiency η . Indeed, its maximum is observed at $Ra = 1000$ with a value of 29.62% which decreases to 10.54% at $Ra = 10000$. This efficiency decrease as a function of Ra has also been noticed by [Farinas et al. \(1997\)](#) in the

case of three fins with a height of 0.5 in an annulus filled with air for the same considered range of Rayleigh number.

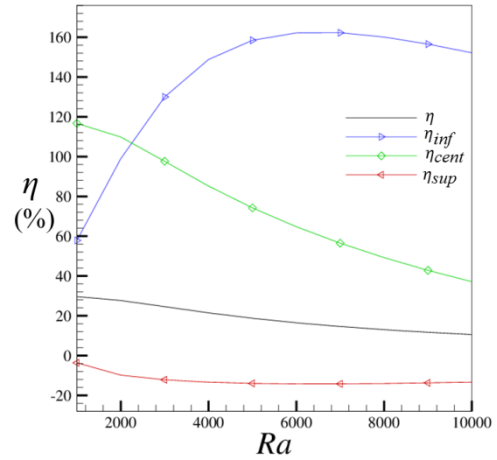


Fig. 10. Efficiency variation as a function of Ra .

4. CONCLUSION

Natural convection in a horizontal annulus with two heating blocks, with inverted trapezoidal shape, placed at a median position, is numerically studied globally and per zone distinguishing three zones: superior, central and inferior. Regardless of Ra , the block presence, which induces a bi-vortex flow, influences positively the overall heat transfer. The detailed analysis of the zones influence on heat transfer shows the following major conclusions:

- As for the without blocks case, the blocks presence shows that the superior vortex, which is intense, gives a higher heat transfer compared to that obtained in the inferior zone.
- Despite this, in comparison with the without blocks configuration, the heat transfer of the superior zone is deteriorated ($\eta_{sup} < 0$), unlike that of the inferior zone which is improved ($\eta_{inf} > 0$).
- The addition of blocks impacts positively heat transfer and enhances it by 10.54% to 29.62%, relatively to the without blocks case, depending on the Rayleigh number that are considered.

ACKNOWLEDGEMENTS

The authors are highly grateful to the reviewers for their valuable suggestions and comments that allowed the improvement of the manuscript.

REFERENCES

Ahmed, H. E. and M. I. Ahmed (2017). Thermal performance of annulus with its applications; A review. *Renewable and Sustainable Energy Reviews* 71, 170-190.

- Alshahrani, D. and O. Zeitoun (2005). Natural convection in horizontal cylindrical annuli with fins. *Alexandria Engineering Journal* 44(6), 825-837.
- Arbaban, M. and M. R. Salimpour (2014). Enhancement of laminar natural convective heat transfer in concentric annuli with radial fins using nanofluids. *Heat Mass Transfer* 51(3), 353-362.
- Bakkas, M., M. Hasnaoui and A. Amahmid (2010). Natural convective flows in horizontal channel provided with heating isothermal blocks: Effect of the inter blocks spacing. *Energy Conversion and Management* 51(2), 296-304.
- Chai, J. C. and S. V. Patankar (1993). Laminar natural convection in internally finned horizontal annulus. *Numerical Heat Transfer Part A: Applications* 24(1), 67-87.
- Charles, R. and C. Wang (2014). A novel heat dissipation fin design applicable for natural convection augmentation. *International Communications in Heat and Mass Transfer* 59, 24-29.
- Cheddadi, A., J. P. Caltagirone, A. Mojtabi and K. Vafai (1992). Free two-dimensional convective bifurcation in a horizontal annulus. *ASME Journal of Heat Transfer* 114(1), 99-106.
- Dawood, H. K., H. A. Mohammed, N. A. Che Sidik, K. M. Munisamy and M. A. Wahid (2015). Forced, natural and mixed-convection heat transfer and fluid flow annulus: A review. *International Communications in Heat and Mass Transfer* 62, 45-57.
- Farinas, M., A. Garon and K. Saint-Louis (1997). Study of heat transfer in a horizontal cylinder with fins. *Revue Générale de Thermique* 36(5), 398-410.
- Ha, M. Y. and J. G. Kim (2004). Numerical simulation of natural convection in annuli with internal fins. *KSME International Journal* 18(4), 718-730.
- Idrissi, A., A. Cheddadi and M. T. Ouazzani (2016). Heat transfer in an annular space fitted with heating isothermal blocks: Numerical bifurcation for low blocks height. *Case studies in Thermal Engineering* 7, 1-7.
- Iqbal, Z., K. S. Syed and M. Ishaq (2011). Optimal convective heat transfer in double pipe with parabolic fins. *International Journal of Heat and Mass Transfer* 54(25-26), 5415-5426.
- Ishaq, M., K. S. Syed, Z. Iqbal, A. Hassan and A. Ali (2013). DG-FEM based simulation of laminar convection in an annulus with triangular fins of different heights. *International Journal of Thermal Sciences* 72, 125-146.
- Kumar, S., K. V. Karanth and K. Murthy (2015). Numerical study of heat transfer in a finned double pipe heat exchanger. *World Journal of Modelling and Simulation* 11(1), 43-54.
- Kundu, B. (2015). Beneficial design of unbaffled shell-and-tube heat exchangers for attachment of longitudinal fins with trapezoidal profile. *Case studies in Thermal Engineering* 5, 104-112.
- Mizushima, J., S. Hayashi and T. Adachi (2001). Transitions of natural convection in a horizontal annulus. *International Journal of Heat and Mass Transfer* 44(6), 1249-1257.
- Nagarani, N., K. Mayilsamy, A. Murugesan and G. S. Kumar (2014). Review of utilization of extended surfaces in heat transfer problems. *Renewable and Sustainable Energy Reviews* 29, 604-613.
- Ould-Amer, Y. (2016). 3D fully developed laminar mixed convection in horizontal concentric annuli with the presence of porous blocks. *IACSIT International Journal of Engineering and Technology* 8(2), 77-82.
- Rahnama, M. and M. Farhadi (2004). Effect of radial fins on two-dimensional turbulent natural convection in a horizontal annulus. *International Journal of Thermal Sciences* 43(3), 255-264.
- Rahnama, M., M. A. Mehrabian, S. H. Mansouri, A. Sinaie and K. Jafargholi (1999). Numerical simulation of laminar natural convection in horizontal annuli with radial fins. *Proceedings of the Institution of Mechanical Engineers, Part E: Journal of Process Mechanical Engineering* 213(2), 93-97.
- Sheikholeslami, M., M. Gorji-Bandpy, I. Pop and S. Soleimani (2013). Numerical study of natural convection between a circular enclosure and a sinusoidal cylinder using control volume based finite element method. *International Journal of Thermal Sciences* 72, 147-158.
- Volkov, K. N. and A. G. Karpenko (2014). Computational modeling of free convection between coaxial cylinders on the basis of a preconditioned form of Navier-Stokes equations. *Journal of Engineering Physics and Thermophysics* 87(4), 929-935.
- Yoo, J. S. (1999). Prandtl number effect on bifurcation and dual solutions in natural convection in a horizontal annulus. *International Journal of Heat and Mass Transfer* 42(17), 3279-3290.
- Yuan, X., F. Tavakkoli and K. Vafai (2015). Analysis of natural convection in horizontal concentric annuli of varying inner shape. *Numerical Heat Transfer Part A: Applications* 68(11), 1155-1174.
- Zhang, L., H. Guo, J. Wu and W. Du (2012). Compound heat transfer enhancement for shell side of double pipe heat exchanger by helical fins and vortex generators. *Heat Mass Transfer* 48(7), 1113-1124.